SCIENCE CHINA
Information Sciences

• LETTER •

June 2026, Vol. 69, Iss. 6, 169401:1–169401:2
https://doi.org/10.1007/s11432-025-4767-6

# A memristor model for high-precision dynamic conductance and its application in neuromorphic computing

Jinhong HU[1], Siyuan SHEN[1], Wen LI[1], Ai CHEN[1], Jiening WU[1], Zhenqi LIU[1], Rui YUAN[1*], Shukai DUAN[1,2,3,4,5*] & Lidan WANG[1,2,3,4,5*]

[1]*College of Artificial Intelligence, Southwest University, Chongqing 400715, China*
[2]*National & Local Joint Engineering Research Center of Intelligent Transmission and Control Technology, Chongqing 400715, China*
[3]*Chongqing Key Laboratory of Brain-inspired Computing and Intelligent Chips, Chongqing 400715, China*
[4]*Key Laboratory of Luminescence Analysis and Molecular Sensing (Southwest University), Ministry of Education, Chongqing 400715, China*
[5]*Chongqing Key Laboratory of Brain-inspired Computing and Intelligent Chips, Chongqing 400715, China*

Received 10 September 2025/Revised 14 December 2025/Accepted 19 January 2026/Published online 8 May 2026

**Citation** Hu J H, Shen S Y, Li W, et al. A memristor model for high-precision dynamic conductance and its application in neuromorphic computing. Sci China Inf Sci, 2026, 69(6): 169401, https://doi.org/10.1007/s11432-025-4767-6

The surge in AI and IoT applications demands high-density, low-power, and cost-effective computational and storage solutions [1]. Memristors, first conceptualized by Chua in 1971 [2], are two-terminal elements whose resistance adapts to charge flow. Widely used in digital circuits and neuromorphic computing, high-fidelity memristor modeling is essential for understanding device characteristics, quantifying noise, and optimizing system reliability.

Various memristor models—including those based on ionic concentration, VTEAM, Bmod, and B6m—all face trade-offs between complexity and accuracy. These models either suffer from excessive parameters without standardized extraction methods, or exhibit poor accuracy with minimal parameters. Yakopcic's model [3] provides a parameter extraction method but exhibits significant shortcomings in simulating synaptic plasticity. Notably, it performs poorly in describing widely used devices such as $Ta_2O_5$ memristors [4], highlighting an urgent need for more precise models to characterize nonvolatile response behavior.

This study proposes a model that accurately simulates the dynamic changes in $Ta_2O_5$-based devices. Based on this model, a human voice recognition application was implemented, attaining an accuracy of 91.6%, thus providing more reliable theoretical support for neuromorphic computing applications.

*Model construction.* The characterization of the $I$-$V$ curve for the model is determined by

$$i(t) = h_1(V(t))x(t) + h_2(V(t))(1 - x(t)), \tag{1}$$

where $h_1$ and $h_2$ represent the electron transport in high-conductance state (HCS) and low-conductance state (LCS), respectively. While HCS often follows near-linear ohmic conduction ($h_1 = \sigma V(t)$) and LCS involves metal-insulator-metal transport, real-world fluctuations typically deviate from pure linearity. To capture this generalized behavior, we define

$$h_1 = g_{max}V(t) + g_{max,flu}V(t)^2, \tag{2}$$

where $g_{max}$ denotes the stable HCS value, while $g_{max,flu}$ represents fluctuation parameters derived from curve fitting. Although the LCS theoretically follows the metal-insulator-metal (MIM) hyperbolic sine model ($\gamma \sinh(\delta V(t))$), significant experimental noise makes this approach difficult to fit. Consequently, we employ a cubic polynomial

$$h_2 = g_{min}V(t) + g_{min,flu_1}V(t)^2 + g_{min,flu_2}V(t)^3 \tag{3}$$

to simplify the fitting process. Eq. (3) defines $g_{min}$ as the stable LCS value, with $g_{min,flu_1}$ and $g_{min,flu_2}$ as fluctuation parameters easily obtained via curve fitting. The $I$-$V$ relationship further depends on the state variable $x(t)$, governed by

$$\frac{dx}{dt} = \eta g(V(t))f(x(t)). \tag{4}$$

In this model, the state variable in (4), which ranges from 0 to 1, directly influences the conductivity. It is jointly determined by two different functions, $g(V(t))$ and $f(x(t))$. We use

$$g(V(t)) = \begin{cases} A_p(e^{V(t)} - e^{V_p}), & V(t) > V_p, \\ -A_n(e^{-V(t)} - e^{V_n}), & V(t) < -V_n, \\ 0, & -V_n \leqslant V(t) \leqslant V_p \end{cases} \tag{5}$$

to describe the threshold voltage. Eq. (5) introduces a threshold voltage, below which state variables remain constant. Once this threshold is exceeded, the state variables evolve according to input polarity via a piecewise function. The ionic motion is modeled by $f(x(t))$, expressed as

$$f(x) = \begin{cases} \alpha_p e^{-(x-x_p)}\omega_p(x, x_p), & x \geqslant x_p, \\ 1, & x \leqslant x_p, \end{cases} \tag{6}$$

* Corresponding author (email: yuanruiswu@swu.edu.cn, duansk@swu.edu.cn, ldwang@swu.edu.cn)

 

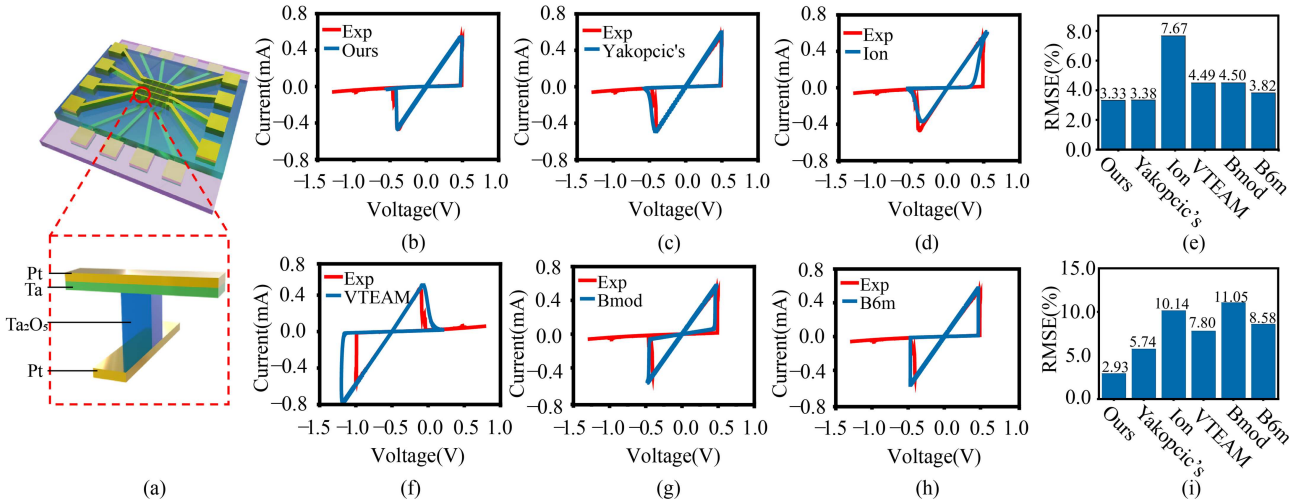


**Figure 1** (Color online) (a) Schematic diagram of cross-array and individual devices; (b) the model used in this paper, (c) Yakopcic's model, and (d) the ion concentration model fitting results; (e) RMSE of the *I*-*V* curve for each model; fitting results for (f) VTEAM, (g) Bmod, and (h) B6m models; (i) comparison of RMSE for the resistive state transition process.

$$f(x)=\begin{cases}\alpha_n e^{(x+x_n-1)}\omega_n(x,x_p,x_n), & x\leqslant 1-x_n,\\ 1, & x\geqslant 1-x_n.\end{cases} \tag{7}$$

The $f(x(t))$ is defined by (6) when $\eta V(t)\geqslant 0$, and by (7) otherwise. Here, $\eta$ indicates voltage polarity: $\eta=1$ when a positive voltage sets the device, and $\eta=-1$ otherwise. Parameters $\alpha_p$ and $\alpha_n$ smooth conductance transitions and broaden the model's applicability, while $x_p$ and $x_n$ define the operational boundaries of window functions $w_p$ and $w_n$:

$$w_p(x,x_p)=\frac{\beta_p(1-x)}{1-x_p}, \tag{8}$$

$$w_n(x,x_p,x_n)=\frac{\beta_n x}{1-x_n+x_p}, \tag{9}$$

where $\beta_p$ and $\beta_n$, as mitigating factors, optimize the characteristics of the *I*-*V* curve in the resistive transition stage by adjusting the window function.

*Comparison of different memristor models.* To validate this model, we employed experimental *I*-*V* data from $Ta_2O_5$ memristors (structure shown in Figure 1(a), preparation details in Appendix A), with the detailed fitting process described in Appendix B. We also compared it with the Yakopcic model, two generalized models, and two recent models (as shown in Figures 1(b)–(d) and Figures 1(f)–(h)). To quantify fitting errors, we employed the root mean square error (RMSE) method detailed in Appendix C for specific comparisons. Figure 1(e) summarizes the global RMSE statistics for all comparative models. The visual data indicate that the proposed model achieves the lowest error across the entire range. We further calculated the RMSE within the resistance transition intervals. As illustrated in Figure 1(i), the proposed model exhibits fitting robustness that far exceeds the other five models, maintaining the RMSE at an exceptionally low level of less than 3% throughout the transient switching regime. Furthermore, we implemented it on the LTspice platform to expand its application scenarios; specific implementation details are provided in Appendix D.

*Application in neuromorphic computing.* We evaluate the potential of the proposed model for real-world applications. The dataset used is a publicly available Chinese speech digit recognition dataset, with details and access provided in Appendix E. In our classification task simulation, memristors serve as electronic synapses, physically storing neural network weights through their non-volatile conductive states. Consequently, weight updates depend on LTP and LTD behaviors within the memristor model. The accuracy rate after simulation training reached 91.6%. For specific training details, please refer to Appendix E.

*Conclusion.* In this study, we propose a novel memristor model that more accurately describes the electrical characteristics of memristors. To explore its practical applications, we applied the model to a speech recognition task, using the memristor model as an analog synapse. Experimental results demonstrated that the model was highly effective in learning and recognizing patterns. These findings suggest that the proposed memristor model has the potential to become a fundamental component of neuromorphic computing systems, paving the way for its application in tasks requiring efficient, hardware-based neural networks.

**Acknowledgements** This work was supported by National Natural Science Foundation of China (Grant Nos. U20A20227, 62076208, 62076207), Chongqing Talent Plan Project (Grant No. CQYC20210302257), Fundamental Research Funds for the Central Universities (Grant Nos. SWU-XDZD22009, SWU-XDJH202319), Chongqing Higher Education Teaching Reform Research Project (Grant No. 211005), Open Fund Project of State Key Laboratory of Intelligent Vehicle Safety Technology (Grant No. IVSTSKL-202309), Youth Fund of the National Natural Science Foundation of China (Grant Nos. 62406260, 62306246), and Key Project of Chongqing Natural Science Foundation Joint Fund (Grant No. CSTB2024NSCQ-LZX0087).

**Supporting information** Appendixes A–E. The supporting information is available online at info.scichina.com and link.springer.com. The supporting materials are published as submitted, without typesetting or editing. The responsibility for scientific accuracy and content remains entirely with the authors.

**References**

1 Ren S G, Dong A W, Yang L, et al. Self-rectifying memristors for three-dimensional in-memory computing. Adv Mater, 2024, 36: 2307218
2 Chua L. Memristor—the missing circuit element. IEEE Trans Circuit Theor, 1971, 18: 507–519
3 Yakopcic C, Taha T M, Mountain D J, et al. Memristor model optimization based on parameter extraction from device characterization data. IEEE Trans Comput-Aided Des Integr Circuits Syst, 2020, 39: 1084–1095
4 Yao L, Ma C, He Z, et al. High-speed $TA_2O_5$-based threshold switching memristor for LIF neurons. J Appl Phys, 2024, 136: 144902